The American Journal of Pathology, Vol. 171, No. 3, September 2007

DOI: 10.2353/ajpath.2007.061029

Tumorigenesis and Neoplastic Progression

Notch2 Signaling Induces Apoptosis and Inhibits Human MDA-MB-231 Xenograft Growth

Christine F. O'Neill, Sumithra Urs, Christina Cinelli, Alexis Lincoln, Robert J. Nadeau, Ruth León, Jessica Toher, Carla Mouta-Bellum, Robert E. Friesel, and Lucy Liaw

From the Center for Molecular Medicine, Maine Medical Center Research Institute, Scarborough, Maine

Notch functions as an oncogene or tumor inhibitor in various cancers, and decreases in Notch2 expression are associated with increasing grade of human breast cancer. We constitutively activated Notch signaling with intracellular domain (ICD) expression in the human adenocarcinoma line MDA-MB-231. Notch2 signaling increased apoptosis, whereas Notch4ICD (*int3*) significantly increased cell proliferation and growth. Cells with activated Notch2 or Notch4 were injected into *nu/nu* mice for analysis of *in vivo* tumor xenograft phenotype. Tumor growth was significantly altered depending on the receptor activated. Notch2ICD potently suppressed tumor take and growth, leading to a 60% decrease in tumors and significantly smaller, necrotic tumors. Despite this, Notch2ICD tumors were highly vascularized, although the vessels were smaller and comprised a more immature network compared with Notch4ICD tumors. Notch4ICD tumors were highly aggressive and well vascularized, indicating a role for Notch4 signaling in the promotion of the malignant phenotype in addition to its transforming ability. Although both NotchICD groups expressed angiogenic factors, Notch4ICD had selective vascular endothelial growth factor-D in both tumor and host stroma, suggesting a differential regulation of cytokines that may impact vascular recruitment and autocrine tumor signaling. Our results demonstrate that Notch2 signaling is a potent inhibitory signal in human breast cancer xenografts. ***(Am J Pathol 2007, 171:1023–1036; DOI: 10.2353/ajpath.2007.061029)***

Notch proteins are transmembrane receptors encoded by four related genes, Notch1 to Notch4.[1–3] Ligand activation of Notch generates the intracellular domain (ICD) that translocates into the nucleus.[4,5] There Notch interacts with members of the CBF1, Su(H), Lag2 domain (CSL) family, activating transcription of a variety of targets including members of the HES/HRT family.[6–8] Normal mammary glands express Notch receptors in the mammary stroma and epithelia,[9] and there is growing evidence that dysregulated Notch activation is associated with cell transformation and tumorigenesis in the mammary gland.[9–11] Recent studies also suggest that Notch signaling plays a role in mammary stem/progenitor cell self-renewal and expansion,[12] which has implications to normal development as well as tumorigenesis.

Activation of Notch signaling in mammary carcinoma has been well studied in mouse models. Activation of Notch1, Notch3, or Notch4 in mouse mammary epithelial cells blocks mammary gland development and leads to mammary tumorigenesis.[9–11] Activated Notch2 in normal mammary epithelial cells *in vivo* has not been reported. In human breast cancer, the potential role of Notch is still unclear, but activated Notch signaling may be common during tumorigenesis. Notch1, Notch4, and Jagged1 are increased in human breast cancer tissue, and high expression of Jagged1 and Notch1 correlated to poor patient survival,[13] suggesting that levels of Notch signaling components may serve as prognostic markers of disease. The accumulation of Notch intracellular domain also correlated to disease recurrence[14] and decreased Numb protein in a variety of breast cancer specimens.[15] In addition, blocking Notch signaling with a general γ-secretase inhibitor, DAPT, or a specific anti-Notch4 antibody decreased mammosphere-forming ability of isolated human ductal carcinoma *in situ* cells.[14] Although these studies suggest that Notch activates an oncogenic pathway in the mammary gland, Notch2 expression is

Supported by National Institutes of Health grant R01 HL070865 (to L.L.) and a grant from the Maine Cancer Foundation (to L.L.) This work was supported by the Pathology Core (K.C. and V.L.), Viral Vector Core Facility (N.C.-C.), and Flow Cytometry Core (M.M., J.M.), which are supported by grants P20RR1555 (to R.E.F. and L.L.) and P20RR018789 (to D.W.) from the National Center for Research Resources. C.C. was supported by a fellowship from the Medical Research Committee of the Maine Medical Center.

Accepted for publication June 8, 2007.

Address reprint requests to Lucy Liaw, Ph.D., Center for Molecular Medicine, Maine Medical Center Research Institute, 81 Research Dr., Scarborough, ME 04076. E-mail: liawl@mmc.org.

associated with better survival in patients with breast cancer, with high expression associated with well-differentiated tumors.[16] These data support the intriguing model that Notch2 activation corresponds to decreased tumor aggressiveness, although causative data linking the Notch2 pathway with mammary tumor phenotype have not been described.

Notch signaling can be clearly oncogenic in some cell types, including the mammary gland.[9,10,17,18] However, equally compelling studies suggest that Notch activation may function to suppress cell transformation or tumorigenesis.[19] For example, Notch1 has been shown to inhibit both mouse skin and human cervical carcinogenesis,[20] and repression of Notch signaling was supportive of fibroblast transformation.[21] Indeed, tumor suppressor activities of Notch have additionally been described in leukemias, lymphomas, myeloma, and cancers of the brain, breast, liver, lung, prostate, and skin. Thus, Notch signaling is very complex and is reflected in distinct activities of ligands, receptors, and the cell-specific context of its activity.

The human mammary adenocarcinoma cell line MDA-MB-231[22] is a useful model for *in vitro* studies and *in vivo* xenografts. It expresses components of Notch signaling pathways, contains transcripts of Notch4 receptor that seem to correspond to an intracellular domain mutant, and accumulates NotchICD, suggesting that endogenous activated Notch may contribute to its phenotype.[17,23] To test the idea that Notch2 activation can inhibit the malignant phenotype, we constitutively activated Notch2 and compared the resultant phenotype with the originally described oncogene *int3*, mouse Notch4ICD. mNotch4ICD was chosen because it is a known oncogene, yet no studies have addressed its direct effect in malignant breast carcinoma. Signaling of each of these pathways was activated using ligand-independent receptors, and our results define an inhibitory role for Notch2 both *in vitro* and in xenografts *in vivo*. Our studies show significant differences in Notch regulation of proliferation, cell survival, effector gene activation, and xenograft growth and vascularization. In addition, we further characterize mNotch4ICD/*int3* in malignant breast carcinoma xenografts, which has not been previously studied. Our experimental models provide insight into potential dynamic effects of Notch signaling in tumors and suggest Notch temporal activity is an important factor in tumor progression.

Materials and Methods

DNA Constructs

Constructs for Notch2 and Notch4 intracellular domain sequences were provided by T. Maciag and I. Prudovsky (Maine Medical Center Research Institute) and used as eukaryotic expression vectors in pcDNA. The human (h) Notch2ICD encodes amino acids 1703 to 2475, contains a V5 tag, and has been extensively characterized.[21,24] The mouse (m) Notch4ICD (*int3*) cDNA was originally obtained from J. Kitajewski (Columbia University, New York, NY).[3] This mNotch4ICD was cloned into the *Sal*I site of pcDNA3.1 and encodes amino acids 1410 to 1958 with an HA epitope tag. Empty vectors were used for transfections to obtain control cell populations. The CBF-1 luciferase construct contains six repeats of the CBF-1 binding sequence, and it and the HRT1 (a generous gift from Eric Olson, University of Texas Southwestern, Dallas, TX) promoter luciferase constructs were used with *Renilla* as a transfection control as described.[23,24]

Cell Culture

BT474, MCF-7, ZR75-1, MDA-MB-468, and MDA-MB- 231 cells were obtained from the American Type Culture Collection (Manassas, VA). BT474 (HTB-20) and MCF-7 (HTB-22) cells were grown in minimal essential medium supplemented with 10% fetal bovine serum and 10 μg/ml insulin. ZR75-1 cells (CRL-1500) were grown in RPMI 1640 medium supplemented with 10% fetal bovine serum. MDA-MB-468 cells (HTB-132) were grown in Leibovitz's L-15 medium supplemented with 10% fetal bovine serum. The MDA-MB-231 cell line HTB-26 was grown in Earle's α-minimal essential medium with glutamine and nucleosides (Mediatech, Herndon, VA) supplemented with 10% fetal bovine serum, 1% nonessential amino acids (Gibco, Invitrogen, Carlsbad, CA), and 50 μg/ml gentamicin (Gibco, Invitrogen). All cells were grown in a humidified 37°C incubator in the presence of 5% carbon dioxide except for the MDA-MB-468 cell line, which was grown in 100% air (0% CO_2). At confluence, cells were subcultured at a 1:4 ratio. MDA-MB-231 cells were stably transfected with expression vectors using GeneJuice (Novagen) and selected with the appropriate resistance antibiotic (200 μg/ml zeocin or 200 μg/ml hygromycin; Invitrogen). Notch2 and Notch4 coexpression was achieved in the MDA-MB-231 cell line by transfecting the hNotch2ICD construct into the established MDA-MB-231 mN4ICD stable line and selecting with zeocin in the presence of maintenance levels of hygromycin. The *in vitro* and *in vivo* experiments were performed using at least three stable cell populations from individual transfections. For knockdown experiments, short hairpin RNA (shRNA) retroviral vectors targeting Notch2 or a nontargeting vector for control were obtained from OpenBiosystems (V2HS_135987; Huntsville, AL). Negative control for transfection was achieved by using the shRNA nonsilencing control vector (RHS_1707), which contains no homology to known mammalian genes. Stable lines were selected with 0.75 μg/ml puromycin. For adenoviral transductions, cells were transduced in serum-free medium with 200 pfu/cell for 4 hours using a LacZ or green fluorescent protein viral construct as a control. For growth curves, cells were plated in complete medium at a concentration of 15,000 to 30,000 cells/cm^2 in 24-well plates and counted on day 1 and then every other day after plating using a Coulter counter. Growth curves were performed with each group measured in quadruplicate, with two counts performed in each well. In some cases, γ-secretase inhibitor XXI (Calbiochem) was added every second day on comparison to a dimethyl sulfoxide control as indi-

cated. For assessment of proliferation, cells were incubated in 10 mmol/L bromodeoxyuridine (BrdU) for 4 hours before fixation in 4% paraformaldehyde and immunostaining or were analyzed for cell cycle phases by flow cytometry following 7-amino-actinomycin D incorporation. Data shown are representative from a minimum of three independent repeats of each experiment. For clonal growth experiments, cells were plated by serial dilution at 100 and 50 cells/well in all six wells of a six-well plate. Two weeks later, cells were washed two times with phosphate-buffered saline (PBS), fixed with methanol, and stained for 10 minutes with toluidine blue (Sigma, St. Louis, MO). Using Scion Image analysis software, a picture of each individual well was taken, the number of colonies were counted, and the total area covered by colonies was calculated. Shown are representative data collected from three independent experiments. Statistical analysis was performed by Student's *t*-test or analysis of variance analysis, as appropriate, and differences were considered statistically significant with $P < 0.05$. For soft agar assays, a layer of 4 ml of 0.8% low-melting temperature agarose (SeaKem) dissolved in MDA-MB-231 growth medium was added to 60-mm dishes and then overlaid with a suspension of cells in 6 ml of 0.4% low-melting temperature agarose. After 21 days, the dishes were stained with 0.1 mg/ml *p*-iodonitrotetrazolium (Sigma) in PBS overnight. The next day, the colonies were counted using a dissecting microscope and pictures taken with a Zeiss AxioCam camera (Carl Zeiss GmbH, Jena, Germany).

Microarray Analysis from Meta-Analysis of Oncomine Database

The expression of Notch2 transcripts in human breast tumor tissues was compared using the Oncomine meta-analysis of cancer gene microarray meta-analysis public database.[25,26] Student's *t*-test was used for analyzing differences between published datasets on the database.

Immunoblotting

Cells were lysed with HNTG buffer [20 mmol/L 4-(2-hydroxyethyl)-1-piperazineethanesulfonic acid, pH 7.4, 150 mmol/L NaCl, 10% glycerol, 1% Triton X-100, 1.5 mmol/L $MgCl_2$, 1.0 mmol/L ethylenediamine tetraacetic acid, protease inhibitor cocktail (Roche), 200 μmol/L $NaVO_4$, 1 mmol/L NaF, and 5 mmol/L β-glycerol phosphate] and cleared of insoluble material by centrifugation for 10 minutes at 14,000 rpm at 4°C. Protein concentration was determined by the bicinchoninic acid method, and 100 μg of protein was loaded. Lysates were subjected to sodium dodecyl sulfate-polyacrylamide gel electrophoresis followed by electrophoretic transfer to nitrocellulose (Schleicher & Schuell, Keene, NH) and immunoblotting with the indicated antibodies. The following antibodies were used for immunoblot analysis: anti-V5 (1:5000; Invitrogen) and anti-HA (1:1000; Covance Research Products, Princeton, NJ) followed by horseradish peroxidase-conjugated secondary antibodies (Bio-Rad, Hercules, CA). Bound antibodies were visualized by chemiluminescence (West Pico SuperSignal; Pierce, Rockford, IL).

Tumor Xenograft Growth in Vivo

All protocols involving mice were evaluated and approved by our Institutional Animal Care and Use Committee and performed under veterinary supervision. NCr homozygous nude mice (Taconic Farms, Germantown, NY) at 5 to 6 weeks of age were injected subcutaneously in the right flank, or in the mammary fat pad, with 2.5×10^6 stably transfected MDA-MB-231 populations. Tumor growth was monitored by palpation, and the onset when tumors were detectable was noted. Tumor size was measured with calipers, and tumor volume was calculated assuming the shape as ellipsoid. Representative data were obtained from five mice per experimental group, and the entire experiment was repeated in three independent trials. Before collection, mice were injected intraperitoneally with 200 μl of 80 mmol/L BrdU solution at 15 hours and 1 hour before collection. Individual tumors were split for fixation in 4% paraformaldehyde and flash freezing in liquid nitrogen and then used for histology and immunostaining or RNA and protein collection, respectively.

Immunostaining

BrdU immunostaining was performed using a monoclonal anti-BrdU antibody (MP Biomedicals, Irvine, CA). Following fixation, cells were treated with 0.3% H_2O_2 in methanol at room temperature for 20 minutes, followed by treatment with 20 μg/ml proteinase K in 50 mmol/L Tris/5 mmol/L ethylenediamine tetraacetic acid for 7 minutes at room temperature. Immediately following proteinase K treatment, cells were washed in 0.4% glycine-PBS and then incubated in 1.5 N HCl for 15 minutes at 37°C. Cells were then washed in 0.1 mol/L borax buffer and immunostained with a 1:100 dilution of anti-BrdU followed by a biotinylated anti-mouse antibody and the ABC Elite reagent. The antigen was detected using diaminobenzidine as the color substrate. Ten random fields of cells were captured for each sample, and the percentage of BrdU-labeled cells was determined by counts of labeled/total cells in a blinded manner. Tumor sections were labeled with biotin dUTP using terminal deoxynucleotidyl transferase (TdT) to detect DNA fragmentation. Following 0.3% H_2O_2 treatment and proteinase K antigen retrieval, tumors were incubated for 1 hour at 37°C in TdT reaction solution [TdT, 0.25 U/μl, biotin-dUTP 0.4 nmol/ml in TdT buffer (30 mmol/L Tris-base pH 7.2, 140 mmol/L sodium cacodylate, and 1 mmol/L cobalt chloride)]. Incubation in TdT reaction termination buffer (300 mmol/L NaCl and 30 mmol/L sodium citrate) quenched TdT activity. Antigen was detected using the ABC Elite reagent and diaminobenzene as the color substrate. Quantitation was done as described for BrdU immunostaining. Immunostaining for endothelial cells was performed with both anti-platelet endothelial cell adhesion molecule (PECAM) antibodies (BD Biosciences, San Jose, CA) and the anti-endothelial antigen MECA-32 (BD Biosciences) with similar results. Anti-PECAM staining was performed with a biotinyltyramide

amplification reagent (Perkin Elmer, Waltham, MA), using diaminobenzidine as the color substrate. Anti-mouse MECA-32 and LYVE-1 antibodies were obtained from R&D Systems (Minneapolis, MN).

Quantification of Vessel Area in Tumor Sections

Noncounterstained PECAM sections (five tumors per condition) were quantified for vessel area. Four or five pictures of comparable regions of each tumor were taken and quantified in a blinded fashion. Using Photoshop 7.0 (Adobe Systems, Mountain View, CA), the vessels were outlined in a transparent layer and filled in with black. The outlined vessel image was opened in Scion Image, converted to binary, thresholded, and the area of black pixels measured. Shown are average percentage of vessel area per tumor area, and results were analyzed by Student's *t*-test to determine statistical significance.

Reverse Transcription-Polymerase Chain Reaction (RT-PCR)

Total RNA was collected using TRI Reagent (Sigma) following the manufacturer's protocol. RNA was reverse-transcribed using random hexamers in the presence of avian myeloblastosis virus reverse transcriptase to make cDNA. Successful cDNA production was verified using primers against glyceraldehyde-3-phosphate dehydrogenase or β-actin. Real-time PCR was performed using SYBR Green for Notch2, HES1, HRT1, and β-actin as the housekeeping gene. cDNA concentration in the samples was adjusted to 50 ng/μl based on the β-actin cDNA content. cDNA (1 μl) and specific primers were added to the SYBR Green PCR master mix (Qiagen, Valencia, CA), and amplification was performed in a Bio-Rad iCycler machine. Shown are relative expression ratios of Notch2, HES1, and HRT1 target genes. For PCR amplification of angiogenic factors in tumors, 25 ng of tumor cDNA was used with human primers and 100 ng of tumor cDNA with mouse primers. Primers used for detection of transcripts for Notch receptors and angiogenic factors can be found in Table 1.

Enzyme-Linked Immunosorbent Assay

Detection of human angiogenic factors in cells was performed using the TransSignal Angiogenesis Antibody Array (Panomics, Fremont, CA) following the manufacturer's instructions. MDA-MB-231 cells were cultured for 24 hours in serum-free medium, medium collected and filtered to remove cellular debris, and 2 ml of undiluted medium was immediately used for the assay.

Mouse Tumor Angiography for Observation of Tumor Vessels

Tumor angiography was performed under terminal anesthesia. Vasodilation buffer (PBS with 4 mg/L papaverin and 1g/L adenosine) was infused into the left ventricle, followed by perfusion fixation with 2% paraformaldehyde/1% glutaraldehyde in PBS. After flushing with PBS to clear fixation solution, bismuth contrast agent mixed 1:1 with 10% gelatin-PBS was injected at 0.2 ml/10 g of body weight. The animal was immediately covered in ice to harden the contrast agent, and X-rays were taken using a specimen radiography system at 25 kV, 3.25 mA for 15 to 30 seconds (Faxitron), and developed using Kodak mammography film.

Results

Notch2 Expression Changes during Human Breast Tumor Progression

Previous studies of human breast cancer showed a correlation of strong Notch2 expression in well-differentiated tumors and determined that Notch2 was associated with

Table 1. Primer Sequences Used in These Studies

Gene	Forward primer	Reverse primer
Cyclophilin (m)	5′-AGCTAGACTTGAAGGGGAATG-3′	5′-ATTTCTTTTGACTTGCGGGC-3′
Cyclophilin (h)	5′-CTCGAATAAGTTTGACTTGTGTTT-3′	5′-CTAGGCATGGGAGGGAACA-3′
Notch1 (m/h)	5′-CTGGGTAGCCATGGGGTGACTC-3′	5′-TGGACCACTTTGCCAACCGGGACAT-3′
Notch2 (m/h)	5′-CACAGAGGCTGGGAAAGGATGATA-3′	5′-GGCCACCTGAAGGGAAGCACATA-3′
Notch3 (m/h)	5′-CCTAGCCCAGCCACTGCCACTG-3′	5′-GTCATGCCTGTGTACTAGGTAC-3′
Notch4 (m)	5′-GCTCTAGAGCTGTGGACCTGATGGGGTGACA-3′	5′-GGGGTACCCCCTAGTTCAGATTTCTT ACAACCGA-3′
HES1 (h)	5′-CTAAACTCCCCAACCCACCT-3′	5′-AGGCGCAATCCAATATGAAC-3′
HRT1 (h)	5′-CGTCGGGATCGGATAAATAA-3′	5′-GCACTCTCGGAATCCTATGC-3′
VEGF-A (m)	5′-CAGAAGGAGAGCAGAAGTCC-3′	5′-CTCCAGGGCTTCATCGTTA-3′
VEGF-A (h)	5′-AAGGAGGAGGGCAGAATCAT-3′	5′-CCAGGCCCTCGTCATTG-3′
VEGF-C (m)	5′-GTAAAAACAAACTTTTCCCTAATTC-3′	5′-TTTAAGGAAGCACTTCTGTGTGT-3′
VEGF-C (h)	5′-AACAAACTCTTCCCCAGCCA-3′	5′-TTTAACAAGCATTTCTGTGGAC-3′
VEGF-D (m)	5′-GCAAGACGAGACTCCACTGC-3′	5′-GGTGCTGAATGAGATCTCCC-3′
VEGF-D (h)	5′-GCAGGAGGAAAATCCACTTG-3′	5′-GGGTGCTGGATTAGATCTTTG-3′
NRP-1 (m)	5′-CCCTGAGAGAGCCACACACA-3′	5′-CGTCACACTCATGCACTGG-3′
NRP-1 (h)	5′-CCCGAGAGAGCCACTCATG-3′	5′-GTCATCACATTCATCCACCAA-3′
NRP-2 (m)	5′-AACTGCAACTTTGATTTTCCG-3′	5′-TGTTCTGTCATTGGGGTTAGC-3′
NRP-2 (h)	5′-CAATTGCAACTTCGATTTCCTC-3′	5′-CCGGTCGTTTGGGCTGGA-3′

h, human; m, mouse.

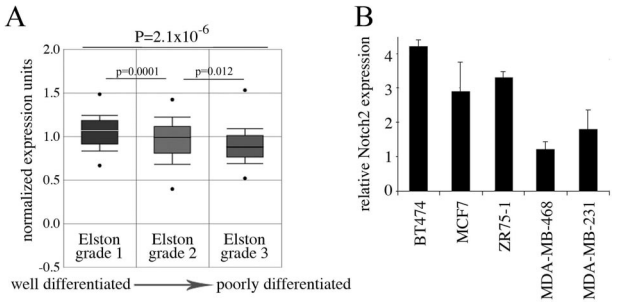

Figure 1. Notch2 expression correlates with tumor aggressiveness in human breast cancer. **A:** Notch2 mRNA levels were analyzed using gene expression data sets from cancer gene microarray meta-analysis database that was originally described by Miller et al.[27] Sixty-seven cases of Elston grade 1, 128 cases of Elston grade 2, and 54 cases of Elston grade 3 were included in this study. The *y* axis represents normalized expression units. Shaded boxes represent interquartile range making the 25th to 75th percentile; whiskers represent the 10th to 90th percent range; bars represent the median. The *P* value was calculated using Student's *t*-test. **B:** Real-time PCR for Notch2 in a panel of human breast tumor cell lines.

better survival outcomes.[16] Because these data suggest a unique role of Notch2 in breast cancer, we used the Oncomine cancer gene microarray meta-analysis public database to query Notch2 levels in human mammary tumors (Figure 1A). Miller et al[27] originally determined gene expression patterns in Elston grade 1 tumors (67 cases), Elston grade 2 tumors (128 tumors), and Elston grade 3 tumors (54 cases). The data show that Notch2 mRNA expression decreases as tumor grade increases, which is consistent with the previous clinical correlation.[16] We assayed several established human mammary tumor cell lines to determine whether Notch2 expression had any relationship to cell source or phenotype (Figure 1B). The BT474 line was derived from a primary ductal carcinoma, whereas the MCF-7, MDA-MB-468, and MDA-MB-231 cells were derived from the pleural effusion of metastatic adenocarcinomas, and the ZR-75-1 line was derived from ascites of a metastatic ductal carcinoma. Real-time PCR showed that the cell line derived from the primary tumor, BT474, demonstrated the highest levels of Notch2, whereas the highly aggressive, metastatic lines showed lower expression levels of Notch2.

Development of Gain and Loss of Function Models of Notch Signaling

Previous studies detected expression of Notch in the MDA-MB-231 cells,[23] and we confirmed detectable protein levels of Notch1, Notch2, Notch4, and the Jagged1 ligand (Figure 2A). To establish a gain-of-function model, the hNotch2 or mNotch4 pathways were stably activated in MDA-MB-231 cells, and NotchICD production was confirmed by Western blotting (Figure 2B). Receptor activity was further validated using a CBF-1 response element as well as HES1 and HRT1 promoter reporters to assess activated Notch signaling (Figure 2C). HES/HRT proteins, in addition to being well-known downstream Notch targets,[28] may participate in the regulation of breast cancer cell growth.[29] Although mNotch4ICD activated CBF-1 reporter and increased HES1 and HRT1 promoter activity, hNotch2ICD activated the CBF1 reporter and increased HES1 promoter activity but did not activate the HRT1 promoter. Quantification of HES1 and HRT steady-state transcript detected HES1 expressed under all conditions, whereas HRT1 was only detected in control and mN4ICD cells (Figure 2D). It is thus possible that hNotch2 signaling has an effect in the repression of HRT1 transcript. Our data show that although NotchICD expression strongly transactivates CBF-1 and HES reporter activity, there is a significant level of HES1 expressed in the control MDA-MB-231 cells, suggesting that endogenous Notch signaling may be active. In addition, treatment of cells with γ-secretase inhibitor decreased cell number in a dose-dependent manner (Figure 2E). Because many genetic studies show that the Notch pathway is very dosage-sensitive, we also generated a loss-of-function model for Notch2 using Notch2 shRNA (Figure 2F) or a nontargeting shRNA. This approach was designed to determine the function of endogenous hNotch2 signaling on tumor cell phenotype. We were able to obtain stable populations of cells with ~50% inhibition of Notch2 transcript for further study.

Notch Regulation of the Malignant Phenotype of MDA-MB-231 Cells in Vitro

Despite the intriguing correlation of Notch2 expression with better prognosis in human patients with breast cancer, there have been few studies addressing the Notch2 pathway in breast cancer cell phenotype. Our analysis thus focused on regulating the Notch2 pathway. Using stable transfectants of NotchICD populations, we found a significant decrease in hNotch2ICD cell number in growth curves *in vitro*, which was a stark contrast to

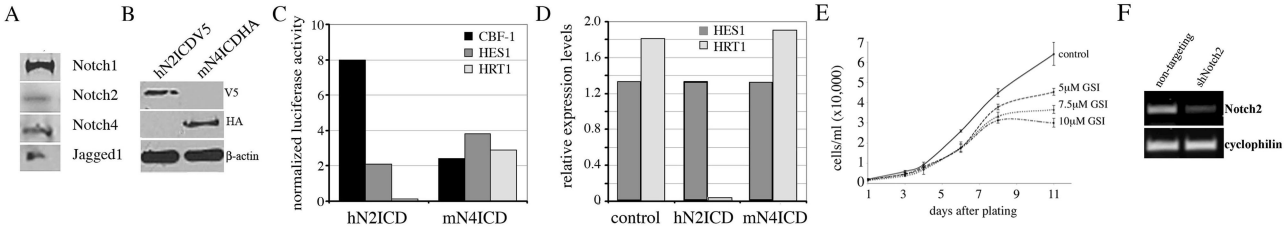

Figure 2. Modulation of Notch signaling in MDA-MB-231 cells. **A:** MDA-MB-231 cell lysates were used for immunoblot using antibodies against the proteins indicated. **B:** Cells were transfected with expression constructs for hNotch2ICD or mNotch4ICD, and proteins were detected by immunoblot using antibodies against the epitope tags. **C:** Stable cell populations were assessed for Notch activation using CBF-1, HES1, and HRT1 luciferase reporter constructs. **D:** Transcript levels of HES1 and HRT1 were determined by real-time PCR. Shown are averages of three independent experiments. **E:** γ-Secretase inhibitor XXI was added every 2 days at the concentrations indicated, and MDA-MB-231 cells were counted up to 11 days after plating. Graphed are means ± SEM analysis of variance analysis at day 11; $P = 0.0013$. **F:** Cells were treated with shRNA to target Notch2 sequences or treated with a nontargeting control. Stable populations were generated with reduced Notch2 transcripts.

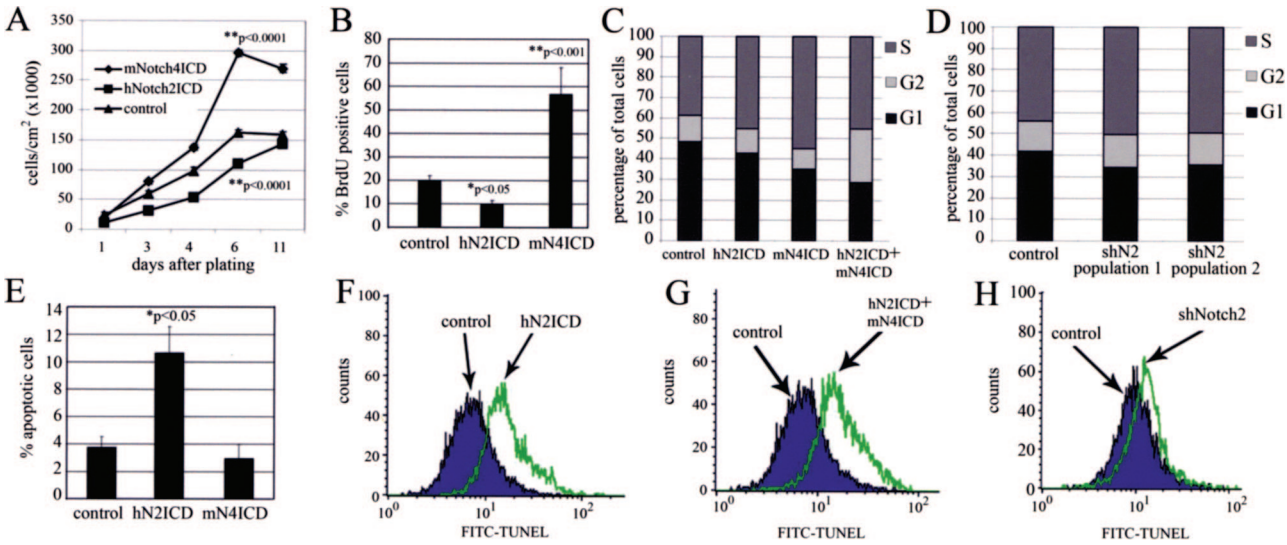

Figure 3. NotchICD affects cell proliferation and apoptosis in MDA-MB-231 stable transfectants. **A:** Cells stably expressing hNotch2ICD or mNotch4ICD were analyzed in a growth curve assay. Cells were plated in 24-well plates at 15,800 cells/cm^2. At days indicated after plating, cells were trypsinized and counted. Values graphed are the average of quadruplicates. **B:** Cultures were pulsed with BrdU and then quantified for BrdU incorporation in each group. Graphed are means ± SEM. **C** and **D:** 7-Amino-actinomycin D incorporation was used for cell cycle analysis of stable populations. Shown are percentages of cells in S, G_2, and G_1 phases. **E–H:** Cells were used for TUNEL labeling to detect apoptotic cells by cell counting (**E**) or flow cytometry (**F–H**). The control in (**H**) is the nontargeting control population. FITC, fluorescein isothiocyanate.

increased growth and cell density of mNotch4ICD populations (Figure 3A). The hNotch2ICD populations had 2.6-fold reduction in cell number (115,000 cells/cm^2) at peak cell density compared with mNotch4ICD cells, which lost their contact inhibition of growth. Quantifying BrdU incorporation, we detected a decrease in hNotch2ICD populations (Figure 3B) and a significant increase in mNotch4ICD cells. Cell cycle analysis using incorporation of 7-amino-actinomycin D was used to compare the cell cycle between groups (Figure 3, C and D). There was a slight difference in percentage of S phase cells in the hNotch2ICD population (45.21%) compared with the control population (38.48%), whereas the mN4ICD cells had a significant 16% increase (54.92%) in S phase cells compared with the control (Figure 3C). When hNotch2ICD and mNotch4ICD were coexpressed, a dramatic increase in cells in G_2 phase was observed (26.32%), whereas the percentage of cells in S phase was similar to hNotch2ICD cells (45.09%). Collectively, these data suggest that the Notch2 pathway alone plays a minor role in MDA-MB-231 proliferation but causes a G_2 block when increased proliferation is stimulated by mNotch4ICD. When endogenous Notch2 levels were decreased using shRNA, the percentage of cells in S phase looked similar to mN4ICD results. Knockdown resulted in 50.17 and 49.43% of cells in S phase in population 1 and population 2 cell lines, respectively (Figure 3D).

Notch2 signaling was then tested for regulation of apoptosis. We used terminal deoxynucleotidyl transferase dUTP nick-end labeling (TUNEL) and quantified either by cell counts (Figure 3E) or by flow cytometry (Figure 3, F–H). In both cases, activation of Notch2 led to increased TUNEL-positive cells, whereas there were no significant changes in TUNEL labeling in Notch4-activated cells. When the Notch2 and the Notch4 pathways were activated together (Figure 3G), there was still activation of apoptosis, similar to the hNotch2ICD alone. Therefore, a major effect of Notch2 activation in the MDA-MB-231 cells is the induction of apoptosis. Knockdown of endogenous Notch2 using shRNA did not have a major effect on TUNEL labeling in these cells (Figure 3H).

A characteristic of a malignant cell is its ability to grow independently of extracellular signals and matrix interactions, and we thus tested cell survival at clonal densities. Activation with hNotch2ICD resulted in decreased colony number (twofold, $P = 0.05$; Figure 4A) and decreased growth area (twofold, $P = 0.05$; not shown). Similarly, Notch2 activation led to a disadvantage in growth in soft agar, with a more than threefold decrease in colony number ($P < 0.05$; not shown). On the other hand, mNotch4ICD cells showed a growth and survival advantage in both assays, with increased adherent growth at clonal density (Figure 4A) and increased soft agar colonies. Several cytokines are known to regulate breast cancer cell growth and survival, including fibroblast growth factor,[30] vascular endothelial growth factor (VEGF),[31,32] hepatocyte growth factor,[33,34] and the interleukins.[35] We thus determined the levels of these cytokines in the conditioned medium of the tumor populations. Surprisingly, all of the cells expressing activated forms of Notch demonstrated higher levels of several factors, and there were no stark differences between Notch2 and Notch4 activation (Figure 4B). Adding conditioned medium from hNotch2ICD or mNotch4ICD populations to MDA-MB-231 parental or empty vector control cells showed no difference in cell growth rates as observed by growth curve analysis (not shown). Therefore, it seemed that a secreted factor was not responsible for the inhibition of survival in hNotch2ICD tumor cells.

To determine the biochemical signaling downstream of NotchICD, we tested cell cycle regulators and signaling pathways. Although some components were unchanged, including the cyclins and phospho-extracellular signal-regulated kinase, we noted significant phospho-AKT and

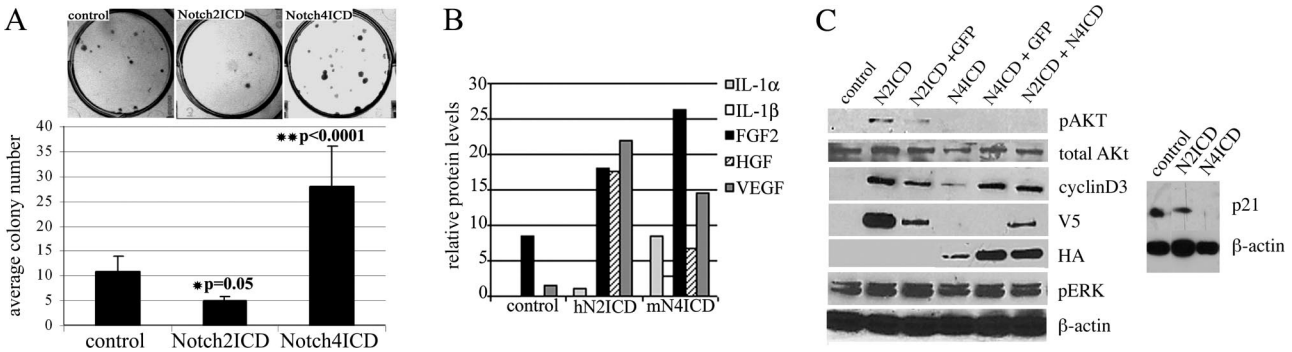

Figure 4. NotchICD affects clonal and anchorage independent growth of MDA-MB-231 cells. **A:** Stably transfected cell populations were plated at clonal growth density at 50 cells/well in a six-well plate. After 2 weeks in culture, cells were fixed in methanol and stained with toluidine blue. Shown are representative wells from each group and the quantitation of average number of colonies/well. Graphed are means ± SEM. Notch2ICD had significantly fewer colonies, and Notch4ICD had significantly more colonies compared with vector transfected controls. **B:** Conditioned medium from stable cell populations was assayed by enzyme-linked immunosorbent assay for levels of the cytokines indicated. **C:** Cell lysates were prepared for immunoblot analysis to detect the proteins listed. hNotch2ICD has a V5 epitope tag, and mNotch4ICD has an HA epitope tag.

p21 expression in the hNotch2ICD group, which were absent in mNotch4ICD (Figure 4C). Thus, in the MDA-MB-231 cells, it seems that p21 may be repressed by mNotch4ICD signaling, corresponding to increased cell cycle transit.

Activation of hNotch2 Inhibits MDA-MB-231 Tumor Xenograft Growth in Vivo

Based on our *in vitro* results, we hypothesized that the increased apoptosis and decreased survival of hNotch2ICD cells would correspond to impaired growth *in vivo*. We used a xenograft model of subcutaneous injection of tumor cells into *nu/nu* mice to assess directly if distinct tumor growth differences were apparent in the cells expressing the NotchICDs and to investigate further if these changes were due to differing angiogenic responses of the tumors. Our first observation was that although the control and the mNotch4ICD animals all formed tumors (100% tumor growth), mice injected with hNotch2ICD had a much lower proportion of tumor take, with ~40% of the animals generating tumors. Even up to 4 months after injection, those animals with unsuccessful hNotch2ICD xenografts did not develop tumors. Second, the growth rate and final size of the tumors in each population was quite distinct. MDA-MB-231 control cells formed significant tumors over the course of 30 to 40 days, whereas the tumors that did develop from hNotch2ICD cells were about fourfold decreased in size (Figure 5, A and B). It was interesting that in the low percentage of tumors that developed from hNotch2ICD cells, the activated Notch2 transgene was no longer detectable at the end of the experiment, even though they were stable transfectants. This observation suggests that the tumor cells with the highest levels of hNotch2ICD

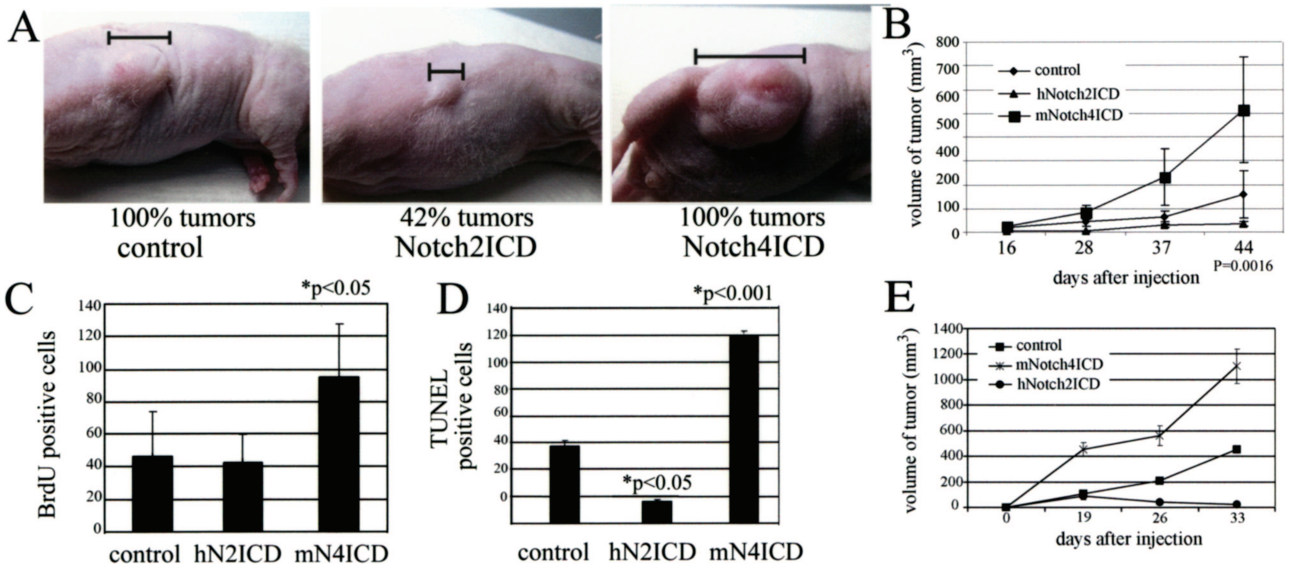

Figure 5. Activation of Notch2 decreases tumor take and tumor growth in xenografts. **A:** MDA-MB-231 cells stably expressing control vector, hNotch2ICD, or mNotch4ICD were grown as xenografts in athymic *nu/nu* mice. Shown are representative mice from each group. **B:** The length and width of the tumors were measured at days indicated, and volumes calculated. Shown are the quantitation of three independent experiments (total, $n = 15$/group) and the corresponding analysis of variance P value. Control and mNotch4ICD cells showed 100% tumor penetrance, whereas the hNotch2ICD cells led to tumors in approximately 40% of the mice. **C:** Cell proliferation was assessed by BrdU incorporation at the end of the experiment, and apoptosis was measured by TUNEL labeling (**D**). **E:** Similar tumor xenograft results were obtained with injection of cells into the mammary fat pad.

were at a survival disadvantage and possibly were overtaken by cells with very low expression or those in which the hNotch2ICD allele was lost or otherwise suppressed. Conversely, the activation of Notch4 led to highly accelerated tumor growth, with approximately threefold increase in tumor size in the same amount of time. Even though an end-stage analysis (at 44 days after injection) cannot reflect tumor cell behavior during the course of xenograft growth, we analyzed BrdU incorporation and TUNEL labeling to quantify proliferation and apoptosis at the end of the experiment. The mN4ICD tumors did have a higher rate of proliferation (Figure 5C), and the level of apoptosis measured by TUNEL labeling (Figure 5D) corresponded to tumor size; there were few TUNEL-positive cells in the hN2ICD tumors, and abundant TUNEL-positive cells in the mN4ICD tumors, probably due to their large size.

Changes in tumor microenvironmental factors influence tumor growth, affecting rates of growth differently dependent on location. This was recently demonstrated for mammary xenografts in particular.[36] To verify that the inhibition of tumor growth by hNotch2ICD was a robust phenomenon, we investigated growth of the same populations in the mammary fat pad. Consistent with subcutaneous growth, Notch2-activated tumor cells were inhibited in the mammary fat pad, and only 25% of the injected mice developed small tumors (Figure 5E). The Notch4-activated cells developed fast-growing, aggressive tumors in all recipients. These observations confirm that the tumor growth inhibition activity of the Notch2 pathway was not specific to one site of xenograft growth.

Pathological Features of NotchICD Xenografts

Tumors were collected for histological analysis and immunostaining. Corresponding to their growth characteristics, we found that the control and hNotch2ICD tumors had necrotic central regions that were filled with inflammatory cells and regions of hemorrhage (Figure 6). Similar features were rare in mNotch4ICD tumors, which had high cell density within the periphery and the core of the tumor. Trichrome staining also demonstrated that hNotch2ICD tumors were fibrotic and had a strong stromal reaction in the tumor, with regions of highly organized vascular networks and fibroblast infiltration between tumor lobes. On the other hand, the mNotch4ICD tumors were more encapsulated and dense, with less apparent collagen content compared with the control tumors.

hNotch2ICD and mNotch4ICD Tumors Have Increased Vascularization

In vitro, the MDA-MB-231 cells expressing activated forms of the Notch receptors secreted increased levels of survival/angiogenic factors. To investigate the ability of these tumors to recruit vessels, markers of blood endothelial (PECAM, MECA-32) and lymphatic endothelial (LYVE-1) cells were used to analyze tumor vascularization (Figure 7). Specific staining of blood vessels was observed in the MECA-32 stained vessels, as adjoining tumor cell-filled lymphatic vessels were not positive (Figure 7A, black arrows). Conversely, LYVE-1 specificity for lymphatic vessels was determined, as adjoining vessels containing blood cells were not positive (Figure 7B, white arrows). We found that the control tumors had a moderate number of blood vessels (Figure 7C) and virtually no lymphatic vessels (Figure 7D). As expected, the aggressive mNotch4ICD tumors had abundant blood and lymphatic vessels within the tumors (Figure 7, G and H). An unexpected finding was that the hNotch2ICD tumors, although small with regions of necrosis, also had a high level of blood and lymphatic vascularization in the tumors (Figure 7, E and F). Blood vessels of the mNotch4ICD tumors were typically found clustered in "hotspots" along the perimeter of the tumors, whereas vessels of hNotch2ICD tumors were present throughout the tissue and were smaller in size. In addition, the lymphatic vessels of both mNotch4ICD and hNotch2ICD tumors were larger with tumor cells completely filling the vessels, in comparison with the blood vessels, which were smaller in diameter and contained blood cells, inflammatory cells, and few tumor cells. This vasculature was functionally linked to the circulation, as shown by X-ray angiography following perfusion into the arterial circulation (Figure 8, A–C). Even though the vasculature in both NotchICD groups was more extensive compared with controls, we did note qualitatively that the tumor vasculature in the hNotch2ICD tumors was composed of much smaller vessels than mNotch4ICD, consistent with the histological analysis. Thus, it is possible that lack of maturity/remodeling of the vessels contributes to the necrosis in the hNotch2ICD tumors. Using PECAM to quantify blood vessels (Figure 8D), we found that hNotch2ICD and mNotch4ICD had an equal area of vascularization per tumor area with a 1.9-fold ($P < 0.0001$) and a 2.3-fold ($P < 0.0001$) increase, respectively, in blood vessel area compared with control tumors. There was a marked increase in the area of lymphatic vessels within the tumor in the hNotch2ICD (twofold, $P < 0.05$) and mNotch4ICD tumors (1.7-fold, $P < 0.001$) compared with control tumors.

Major angiogenic/lymphangiogenic regulators are members of the fibroblast growth factor[37] and VEGF families, which are major therapeutic targets for breast cancer.[38] To determine whether Notch signaling affects these vascular cytokines, human-specific and mouse-specific RT-PCR primers were generated to identify cytokines from the human tumor cells versus the mouse host within the tumors. This analysis was done using RNA collected from tumors at the end of the experiment (44 days after injection). In terms of tumor-derived transcripts (human primers), hNotch2ICD tumors only expressed VEGF-A among VEGF members and did not express Ang1 (not shown) or the neuropilins, unlike the control and mNotch4ICD tumors. The mNotch4ICD tumors selectively expressed VEGF-C and VEGF-D but did not express fibroblast growth factor-1, which was found in control and hNotch2ICD tumors (Figure 8E). From the tumor stroma (Figure 8F), we could detect mouse transcripts encoding for VEGF-D selectively in the mNotch4ICD tumors and neuropilin-1 in both NotchICD tumors.

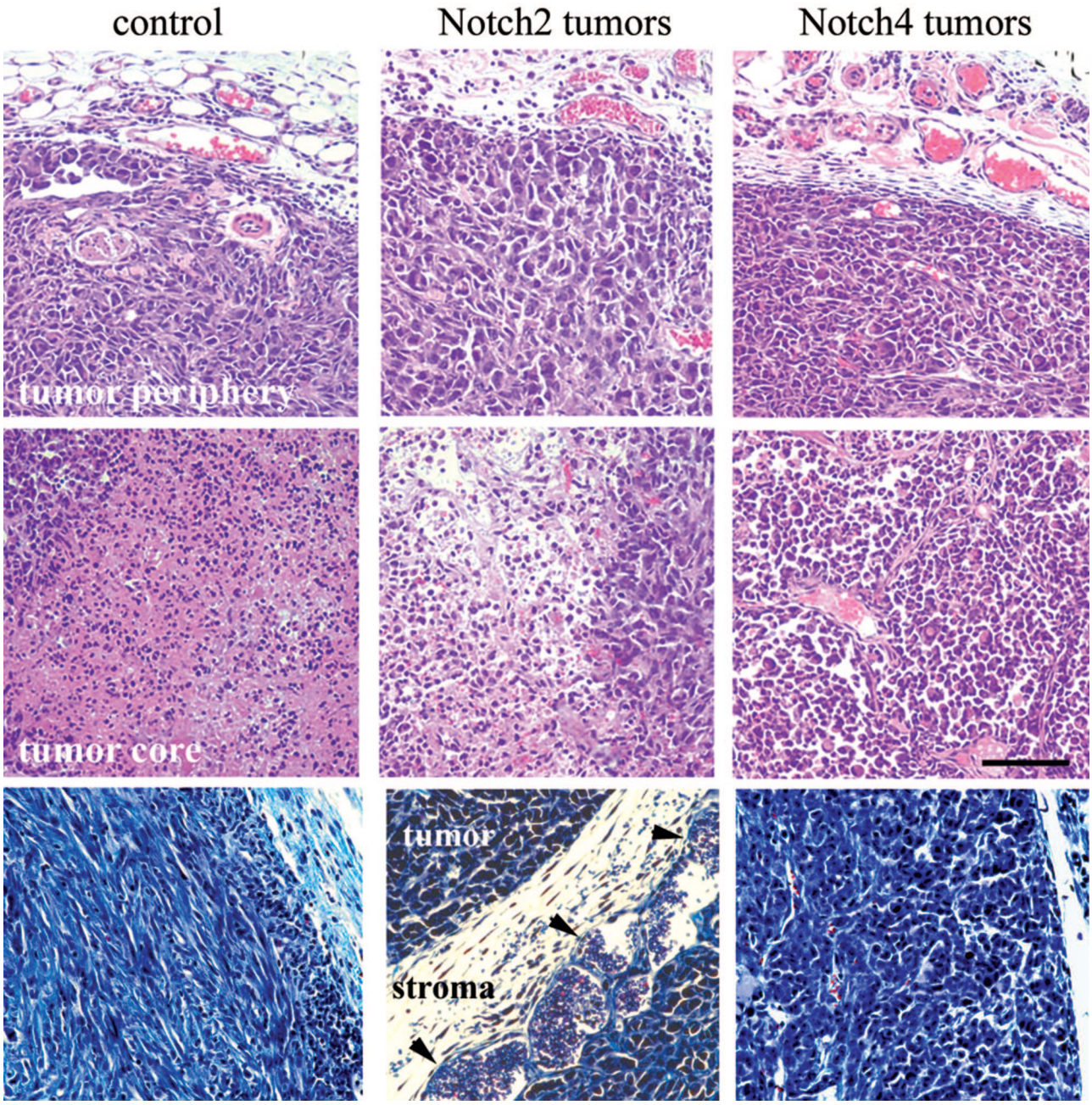

Figure 6. Histological features of NotchICD xenografts. Tumors were collected at 44 days after injection, and processed for hematoxylin and eosin staining (top two rows) or Masson's trichrome staining (bottom row). Representative pictures are shown from the tumor periphery below the skin (top) and the tumor core (middle). Scale bar = 100 μm in all panels.

Discussion

Notch Signaling in Breast Cancer

There has been a recent surge of interest in Notch as a therapeutic target for cancer,[39–41] although the controversial nature of Notch as an oncogene versus a tumor inhibitor is important to consider.[19] In mouse models, activation of Notch1, Notch3, or Notch4 leads to transformation of mammary epithelial cells and tumorigenesis,[9–11] yet few studies have addressed Notch signaling in malignant breast cancer cells. Understanding Notch regulation of malignant breast cancer is relevant to therapeutics, because treatments attempt to stop tumor progression and angiogenesis rather than target initial transformation events that are clinically unpredictable. In studies of human breast cancer, it is difficult to distinguish between Notch as a transforming stimulus or as a marker/promoter of malignant tumor progression except in cases where germline or somatic mutations are discovered.[42–44] Pece et al[15] and Stylianou et al[17] have shown that reducing Notch signaling reverts the transformed phenotype of primary breast cancer cells and breast cancer cell lines, respectively. Both of these results suggest that Notch signaling is required for the

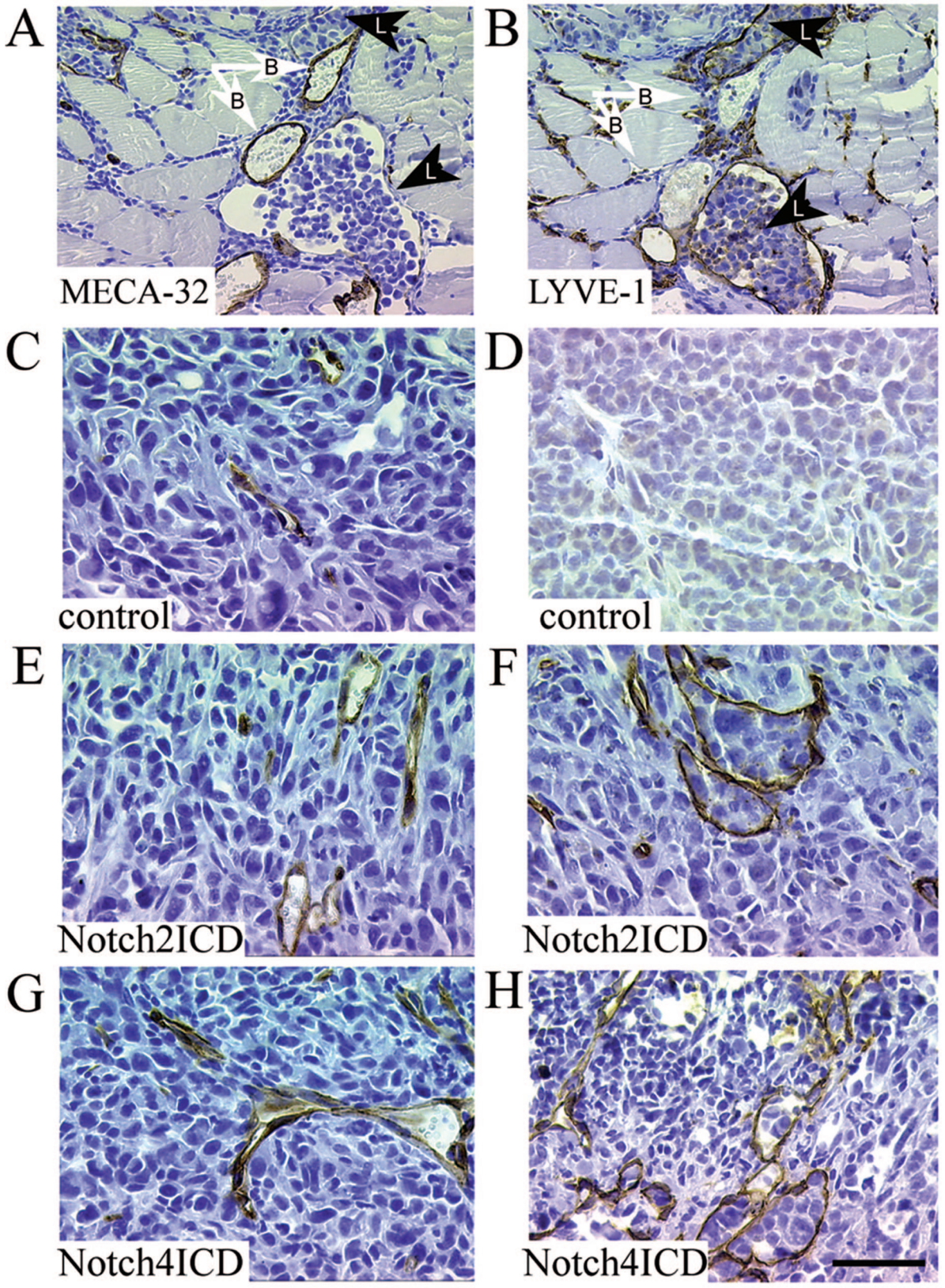

Figure 7. NotchICD tumors have different patterns of vascularization. MECA-32 (**A**, **C**, **E**, and **G**) and LYVE-1 (**B**, **D**, **F**, and **H**) staining was used to determine the presence of blood and lymphatic vessels within tumor sections. As shown in serial sections (**A** and **B**), these two antibodies showed a nonoverlapping pattern of staining, with MECA-32 recognizing red blood cell-filled blood vessels that are not stained with anti-LYVE-1 (**white arrows**). Conversely, lymphatic vessels (L) were stained prominently with anti-LYVE-1 but not MECA-32 (**black arrowheads**). Tumor cells were found frequently within lymphatic vessels. Sections were counterstained with hematoxylin. Scale bars: 50 μm (**A** and **B**); 100 μm (**C–H**).

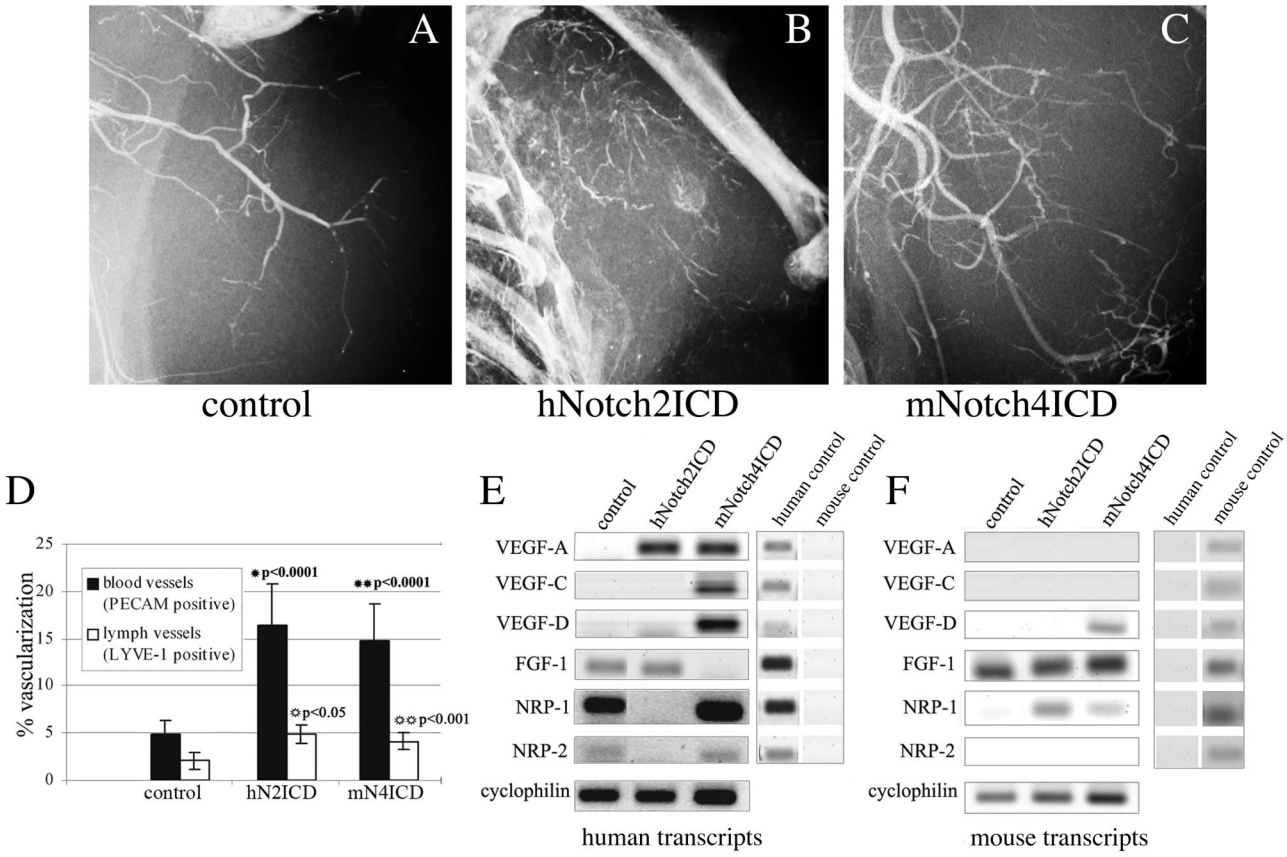

Figure 8. Vascularization and angiogenic cytokine expression of NotchICD xenografts. **A–C:** Tumor-bearing mice were perfused with bismuth for X-ray angiography. **D:** MDA-MB-231 tumors stably expressing NotchICD were collected, fixed, and stained using PECAM (black bars) to detect blood vessels and LYVE-1 (white bars) to detect lymphatic vessels. The percentage of area covered with vessels in each case was quantified, and shown are means ± SEM. Both Notch2ICD and Notch4ICD tumors show an increase in tumor vascularization. **E** and **F:** RT-PCR was used to determine transcript levels of angiogenic cytokines in the tumors. Primers were designed specifically to detect tumor-derived human (**E**) versus host-derived mouse transcripts (**F**).

transformed phenotype, although they do not indicate when Notch signaling is activated. It is of interest to note recent correlation of Notch2 expression with more differentiated tumors and better survival outcome in patients with breast cancer.[16] This is in contrast to activated Notch1 found in human breast carcinoma[17] and high levels of Jagged1 and Notch1[16] associating with poorer overall patient survival.[13] Our results support the model that Notch2 activation plays a role in the inhibition of mammary adenocarcinoma growth.

Tissue Selectivity of Notch Pathways in Tumor Phenotype

Our discovery that Notch2 signaling in the MDA-MB-231 system leads to tumor inhibition may be tissue type-selective. Previous studies have shown that Notch2 is oncogenic in thymic lymphoma[45] and that, in embryonal brain tumor cell lines, Notch2 increases tumorigenicity, whereas Notch1 suppresses tumorigenicity.[46] Furthermore, Notch2 signaling led to growth arrest of small cell lung cancer cells[47] but was transforming in rat kidney cells.[18] These collective data imply that the cellular context of Notch2 signaling is critical for tumorigenic outcome, as is apparently the case for all Notch receptors.[19] In addition, other oncogenic stimuli such as activated Wnt signaling,[48] activated Ras,[49] and myc activity[50] may modify the effects of Notch signaling on breast cancer phenotype. If substantiated by further studies, the balance of signaling through independent Notch receptors will be a critical consideration in designing Notch inhibitors as a therapeutic strategy for breast cancer.

Mechanisms of Notch Activity in Breast Cancer Xenografts

One of our findings was that the Notch effector HRT1 is repressed selectively in the hNotch2ICD cultures. This is of interest, because the HES/HRT families have been shown to target cell cycle regulators. Notch regulates tumor cell proliferation through regulation of cyclin D1 and the cdk inhibitors $p27^{kip}$ and $p21^{WAF1/Cip1}$,[51] and we have observed that $p27^{kip}$ is a direct transcriptional target of HRT2.[52] Sriuranpong et al[48] have demonstrated that Notch1 and Notch2 activity in small cell lung cancer cells results in significant growth arrest and apoptosis. The inhibition of these cancer cells was a result of up-regulation of $p27^{kip}$ concomitant with G_1 cell cycle inhibition. Although we did address the regulation of these cyclin-dependent kinase inhibitors and cyclin-dependent kinases in our model, we found that none of our cells or

tumors express detectable $p27^{kip}$, as previously reported.[51] However, $p21^{WAF1/Cip1}$ was repressed by mNotch4ICD, and this may contribute to cell cycle progression in these cells. Interestingly, the Notch2-activated cells forced a G_2 arrest when this pathway was activated concomitantly with Notch4 activation, which is a similar effect of chemotherapeutic drugs on breast cancer cells. However, unlike some of these drug mechanisms,[53] Notch signaling is not mediated by extracellular signal-regulated kinase phosphorylation, although loss of AKT phosphorylation in the Notch2ICD/Notch4ICD compared with Notch2ICD alone may contribute to an AKT-dependent cascade. The caveat to these experiments and interpreting their connection to the *in vivo* phenotype is that dynamic changes in cell cycle components occur during tumor progression in the host microenvironment that cannot be mimicked *in vitro*. However, our results provide evidence that activation of multiple Notch pathways leads to phenotypes distinct from either pathway alone and that the mechanisms may not be limited to regulation of cell cycle components.

Tumor Growth in Vivo*: Regulation of Tumor Size and Tumor/Host Interactions by Notch*

The ability of a tumor to interact with the surrounding stroma is essential to tumor progression. One interaction is with stromal endothelium, and Notch is required for proper vascular development and physiological angiogenesis.[54] Correlation between Notch signaling and angiogenesis/lymphangiogenesis was demonstrated in squamous cell carcinoma[55] and a breast tumor model.[56] In our studies, where Notch was activated in the tumor cells and not the vasculature, tumors expressing hNotch2ICD grew slowly and were apoptotic, although they were highly vascularized. However, hNotch2ICD tumors had large numbers of small vessels, whereas mNotch4ICD tumors showed a mature network of large vessels, suggesting that lack of maturity/remodeling may contribute to necrosis in the hNotch2ICD tumors. Interestingly, recent studies of the Notch ligand delta-like ligand 4 (Dll4) show that Dll4 inhibition leads to excessive angiogenic branching and sprouting, although the resultant vessels were immature, and in the context of tumors, led to decreased tumor growth.[57–59] Our studies are consistent with these studies in showing that tumor growth may be independent from vessel density, and the collective data show that modulation of Notch signaling in either tumor or stromal compartments affects tumor phenotype through regulation of the tumor vasculature. Studies of human breast cancer samples found that intratumoral microvessel density did not associate with other biological markers such as p53 status, c-erbB-2 protein, or cell cycle kinetics; however, intratumoral vessel density and tumor size were significant but independent predictors of overall survival of patients.[60]

In summary, our study demonstrates that activation of different Notch receptors in the human mammary adenocarcinoma cell line MDA-MB-231 leads to dramatically opposing effects, leading to either increased apoptosis in the case of Notch2 or increased proliferation in the case of Notch4. Furthermore, *in vivo* xenografts are significantly repressed by Notch2 activation, leading to limited tumor formation and small, necrotic tumors. Our studies are the first to show that direct activation of the Notch2 pathway reduces tumorigenicity in human breast cancer xenografts and that Notch4 activation increases malignancy *in vivo*. Our findings suggest that each Notch signaling pathway has a distinct role in breast tumor progression. Therefore, our studies provide novel information regarding differences in Notch receptor signaling in human breast cancer cells and provide a basis for understanding the structural and signal mediators of these pathways.

Acknowledgments

We thank Dr. Michael Jones (Maine Medical Center) for pathological analysis of tumor xenografts, Katie Schlieper and Sarah Himmelfarb for assistance in image analysis and quantitation, and the laboratories of Igor Prudovsky (Maine Medical Center Research Institute), Eric Olson (University of Texas Southwestern Medical Center), and Jan Kitajewski (Columbia University) for sharing reagents.

References

1. del Amo FF, Gendron-Maguire M, Swiatek PJ, Jenkins NA, Copeland NG, Gridley T: Cloning, analysis, and chromosomal localization of Notch-1, a mouse homolog of Drosophila Notch. Genomics 1993, 15:259–264
2. Lardelli M, Lendahl U: Motch A and motch B: two mouse Notch homologues coexpressed in a wide variety of tissues. Exp Cell Res 1993, 204:364–372
3. Uyttendaele H, Marazzi G, Wu G, Yan Q, Sassoon D, Kitajewski J: Notch4/int-3, a mammary proto-oncogene, is an endothelial cell-specific mammalian Notch gene. Development 1996, 122:2251–2259
4. Mumm JS, Schroeter EH, Saxena MT, Griesemer A, Tian X, Pan DJ, Ray WJ, Kopan R: A ligand-induced extracellular cleavage regulates γ-secretase-like proteolytic activation of Notch1. Mol Cell 2000, 5:197–206
5. Brou C, Logeat F, Gupta N, Bessia C, LeBail O, Doedens JR, Cumano A, Roux P, Black RA, Israel A: A novel proteolytic cleavage involved in Notch signaling: the role of the disintegrin-metalloprotease TACE. Mol Cell 2000, 5:207–216
6. Struhl G, Fitzgerald K, Greenwald I: Intrinsic activity of the Lin-12 and Notch intracellular domains in vivo. Cell 1993, 74:331–345
7. Rebay I, Fehon RG, Artavanis-Tsakonas S: Specific truncations of Drosophila Notch define dominant activated and dominant negative forms of the receptor. Cell 1993, 74:319–329
8. Schroeter EH, Kisslinger JA, Kopan R: Notch-1 signalling requires ligand-induced proteolytic release of intracellular domain. Nature 1998, 393:382–386
9. Smith GH, Gallahan D, Diella F, Jhappan C, Merlino G, Callahan R: Constitutive expression of a truncated INT3 gene in mouse mammary epithelium impairs differentiation and functional development. Cell Growth Differ 1995, 6:563–577
10. Jhappan C, Gallahan D, Stahle C, Chu E, Smith GH, Merlino G, Callahan R: Expression of an activated Notch-related int-3 transgene interferes with cell differentiation and induces neoplastic transformation in mammary and salivary glands. Genes Dev 1992, 6:345–355
11. Hu C, Dievart A, Lupien M, Calvo E, Tremblay G, Jolicoeur P: Overexpression of activated murine Notch1 and Notch3 in transgenic mice blocks mammary gland development and induces mammary tumors. Am J Pathol 2006, 168:973–990
12. Dontu G, Jackson KW, McNicholas E, Kawamura MJ, Abdallah WM, Wicha MS: Role of Notch signaling in cell-fate determination of human mammary stem/progenitor cells. Breast Cancer Res 2004, 6:R605–R615
13. Reedijk M, Odorcic S, Chang L, Zhang H, Miller N, McCready DR, Lockwood G, Egan SE: High-level coexpression of JAG1 and NOTCH1 is observed in human breast cancer and is associated with poor overall survival. Cancer Res 2005, 65:8530–8537

14. Farnie G, Clarke RB, Spence K, Pinnock N, Brennan K, Anderson NG, Bundred NJ: Novel cell culture technique for primary ductal carcinoma in situ: role of Notch and epidermal growth factor receptor signaling pathways. J Natl Cancer Inst 2007, 99:616–627
15. Pece S, Serresi M, Santolini E, Capra M, Hulleman E, Galimberti V, Zurrida S, Maisonneuve P, Viale G, Di Fiore PP: Loss of negative regulation by Numb over Notch is relevant to human breast carcinogenesis. J Cell Biol 2004, 167:215–221
16. Parr C, Watkins G, Jiang WG: The possible correlation of Notch-1 and Notch-2 with clinical outcome and tumour clinicopathological parameters in human breast cancer. Int J Mol Med 2004, 14:779–786
17. Stylianou S, Clarke RB, Brennan K: Aberrant activation of notch signaling in human breast cancer. Cancer Res 2006, 66:1517–1525
18. Capobianco AJ, Zagouras P, Blaumueller CM, Artavanis-Tsakonas S, Bishop JM: Neoplastic transformation by truncated alleles of human NOTCH1/TAN1 and NOTCH2. Mol Cell Biol 1997, 17:6265–6273
19. Leong KG, Karsan A: Recent insights into the role of Notch signaling in tumorigenesis. Blood 2006, 107:2223–2233
20. Rangarajan A, Talora C, Okuyama R, Nicolas M, Mammucari C, Oh H, Aster JC, Krishna S, Metzger D, Chambon P, Miele L, Aguet M, Radtke F, Dotto GP: Notch signaling is a direct determinant of keratinocyte growth arrest and entry into differentiation. EMBO J 2001, 20:3427–3436
21. Small D, Kovalenko D, Kacer D, Liaw L, Landriscina M, Di Serio C, Prudovsky I, Maciag T: Soluble Jagged 1 represses the function of its transmembrane form to induce the formation of the Src-dependent chord-like phenotype. J Biol Chem 2001, 276:32022–32030
22. Cailleau R, Olive M, Cruciger QV: Long-term human breast carcinoma cell lines of metastatic origin: preliminary characterization. In Vitro 1978, 14:911–915
23. Imatani A, Callahan R: Identification of a novel NOTCH-4/INT-3 RNA species encoding an activated gene product in certain human tumor cell lines. Oncogene 2000, 19:223–231
24. Small D, Kovalenko D, Soldi R, Mandinova A, Kolev V, Trifonova R, Bagala C, Kacer D, Battelli C, Liaw L, Prudovsky I, Maciag T: Notch activation suppresses fibroblast growth factor-dependent cellular transformation. J Biol Chem 2003, 278:16405–16413
25. Rhodes DR, Yu J, Shanker K, Deshpande N, Varambally R, Ghosh D, Barrette T, Pandey A, Chinnaiyan AM: ONCOMINE: a cancer microarray database and integrated data-mining platform. Neoplasia 2004, 6:1–6
26. Rhodes DR, Yu J, Shanker K, Deshpande N, Varambally R, Ghosh D, Barrette T, Pandey A, Chinnaiyan AM: Large-scale meta-analysis of cancer microarray data identifies common transcriptional profiles of neoplastic transformation and progression. Proc Natl Acad Sci USA 2004, 101:9309–9314
27. Miller LD, Smeds J, George J, Vega VB, Vergara L, Ploner A, Pawitan Y, Hall P, Klaar S, Liu ET, Bergh J: An expression signature for p53 status in human breast cancer predicts mutation status, transcriptional effects, and patient survival. Proc Natl Acad Sci USA 2005, 102:13550–13555
28. Iso T, Kedes L, Hamamori Y: HES and HERP families: multiple effectors of the Notch signaling pathway. J Cell Physiol 2003, 194:237–255
29. Hartman J, Muller P, Foster JS, Wimalasena J, Gustafsson JA, Strom A: HES-1 inhibits 17β-estradiol and heregulin-β1-mediated upregulation of E2F-1. Oncogene 2004, 23:8826–8833
30. Korah R, Choi L, Barrios J, Wieder R: Expression of FGF-2 alters focal adhesion dynamics in migration-restricted MDA-MB-231 breast cancer cells. Breast Cancer Res Treat 2004, 88:17–28
31. Mercurio AM, Lipscomb EA, Bachelder RE: Non-angiogenic functions of VEGF in breast cancer. J Mammary Gland Biol Neoplasia 2005, 10:283–290
32. Wu Y, Hooper AT, Zhong Z, Witte L, Bohlen P, Rafii S, Hicklin DJ: The vascular endothelial growth factor receptor (VEGFR-1) supports growth and survival of human breast carcinoma. Int J Cancer 2006, 119:1519–1529
33. Fan S, Ma YX, Wang JA, Yuan RQ, Meng Q, Cao Y, Laterra JJ, Goldberg ID, Rosen EM: The cytokine hepatocyte growth factor/scatter factor inhibits apoptosis and enhances DNA repair by a common mechanism involving signaling through phosphatidyl inositol 3′ kinase. Oncogene 2000, 19:2212–2223
34. Qiao H, Saulnier R, Patryzkat A, Rahimi N, Raptis L, Rossiter J, Tremblay E, Elliott B: Cooperative effect of hepatocyte growth factor and fibronectin in anchorage-independent survival of mammary carcinoma cells: requirement for phosphatidylinositol 3-kinase activity. Cell Growth Differ 2000, 11:123–133
35. Nicolini A, Carpi A, Rossi G: Cytokines in breast cancer. Cytokine Growth Factor Rev 2006, 17:325–337
36. Monsky WL, Mouta Carreira C, Tsuzuki Y, Gohongi T, Fukumura D, Jain RK: Role of host microenvironment in angiogenesis and microvascular functions in human breast cancer xenografts: mammary fat pad versus cranial tumors. Clin Cancer Res 2002, 8:1008–1013
37. Presta M, Dell'Era P, Mitola S, Moroni E, Ronca R, Rusnati M: Fibroblast growth factor/fibroblast growth factor receptor system in angiogenesis. Cytokine Growth Factor Rev 2005, 16:159–178
38. Schneider BP, Sledge GW Jr: Drug insight: VEGF as a therapeutic target for breast cancer. Nat Clin Pract Oncol 2007, 4:181–189
39. Shi W, Harris AL: Notch signaling in breast cancer and tumor angiogenesis: cross-talk and therapeutic potentials. J Mammary Gland Biol Neoplasia 2006, 11:41–52
40. Miele L, Miao H, Nickoloff BJ: NOTCH signaling as a novel cancer therapeutic target. Curr Cancer Drug Targets 2006, 6:313–323
41. Shih Ie M, Wang TL: Notch signaling, gamma-secretase inhibitors, and cancer therapy. Cancer Res 2007, 67:1879–1882
42. Callahan R, Smith GH: MMTV-induced mammary tumorigenesis: gene discovery, progression to malignancy and cellular pathways. Oncogene 2000, 19:992–1001
43. Park JT, Li M, Nakayama K, Mao TL, Davidson B, Zhang Z, Kurman RJ, Eberhart CG, Shih Ie M, Wang TL: Notch3 gene amplification in ovarian cancer. Cancer Res 2006, 66:6312–6318
44. Zhu YM, Zhao WL, Fu JF, Shi JY, Pan Q, Hu J, Gao XD, Chen B, Li JM, Xiong SM, Gu LJ, Tang JY, Liang H, Jiang H, Xue YQ, Shen ZX, Chen Z, Chen SJ: NOTCH1 mutations in T-cell acute lymphoblastic leukemia: prognostic significance and implication in multifactorial leukemogenesis. Clin Cancer Res 2006, 12:3043–3049
45. Rohn JL, Lauring AS, Linenberger ML, Overbaugh J: Transduction of Notch2 in feline leukemia virus-induced thymic lymphoma. J Virol 1996, 70:8071–8080
46. Fan X, Mikolaenko I, Elhassan I, Ni X, Wang Y, Ball D, Brat DJ, Perry A, Eberhart CG: Notch1 and notch2 have opposite effects on embryonal brain tumor growth. Cancer Res 2004, 64:7787–7793
47. Sriuranpong V, Borges MW, Ravi RK, Arnold DR, Nelkin BD, Baylin SB, Ball DW: Notch signaling induces cell cycle arrest in small cell lung cancer cells. Cancer Res 2001, 61:3200–3205
48. Ayyanan A, Civenni G, Ciarloni L, Morel C, Mueller N, Lefort K, Mandinova A, Raffoul W, Fiche M, Dotto GP, Brisken C: Increased Wnt signaling triggers oncogenic conversion of human breast epithelial cells by a Notch-dependent mechanism. Proc Natl Acad Sci USA 2006, 103:3799–3804
49. Fitzgerald K, Harrington A, Leder P: Ras pathway signals are required for notch-mediated oncogenesis. Oncogene 2000, 19:4191–4198
50. Klinakis A, Szabolcs M, Politi K, Kiaris H, Artavanis-Tsakonas S, Efstratiadis A: Myc is a Notch1 transcriptional target and a requisite for Notch1-induced mammary tumorigenesis in mice. Proc Natl Acad Sci USA 2006, 103:9262–9267
51. Craig C, Wersto R, Kim M, Ohri E, Li Z, Katayose D, Lee SJ, Trepel J, Cowan K, Seth P: A recombinant adenovirus expressing p27Kip1 induces cell cycle arrest and loss of cyclin-Cdk activity in human breast cancer cells. Oncogene 1997, 14:2283–2289
52. Havrda MC, Johnson MJ, O'Neill CF, Liaw L: A novel mechanism of transcriptional repression of p27kip1 through Notch/HRT2 signaling in vascular smooth muscle cells. Thromb Haemost 2006, 96:361–370
53. Zheng A, Kallio A, Harkonen P: Tamoxifen-induced rapid death of MCF-7 Breast cancer cells is mediated via ERK signaling and can be abrogated by estrogen. Endocrinology 2007,148:2764–2777
54. Krebs LT, Xue Y, Norton CR, Shutter JR, Maguire M, Sundberg JP, Gallahan D, Closson V, Kitajewski J, Callahan R, Smith GH, Stark KL, Gridley T: Notch signaling is essential for vascular morphogenesis in mice. Genes Dev 2000, 14:1343–1352
55. Zeng Q, Li S, Chepeha DB, Giordano TJ, Li J, Zhang H, Polverini PJ, Nor J, Kitajewski J, Wang CY: Crosstalk between tumor and endothelial cells promotes tumor angiogenesis by MAPK activation of Notch signaling. Cancer Cell 2005, 8:13–23
56. Soares R, Balogh G, Guo S, Gartner F, Russo J, Schmitt F: Evidence for the notch signaling pathway on the role of estrogen in angiogenesis. Mol Endocrinol 2004, 18:2333–2343
57. Ridgway J, Zhang G, Wu Y, Stawicki S, Liang WC, Chanthery Y,

Kowalski J, Watts RJ, Callahan C, Kasman I, Singh M, Chien M, Tan C, Hongo JA, de Sauvage F, Plowman G, Yan M: Inhibition of Dll4 signalling inhibits tumour growth by deregulating angiogenesis. Nature 2006, 444:1083–1087

58. Thurston G, Noguera-Troise I, Yancopoulos GD: The Delta paradox: dLL4 blockade leads to more tumour vessels but less tumour growth. Nat Rev Cancer 2007, 7:327–331
59. Noguera-Troise I, Daly C, Papadopoulos NJ, Coetzee S, Boland P, Gale NW, Lin HC, Yancopoulos GD, Thurston G: Blockade of Dll4 inhibits tumour growth by promoting non-productive angiogenesis. Nature 2006, 444:1032–1037
60. Bevilacqua P, Barbareschi M, Verderio P, Boracchi P, Caffo O, Dalla Palma P, Meli S, Weidner N, Gasparini G: Prognostic value of intratumoral microvessel density, a measure of tumor angiogenesis, in node-negative breast carcinoma: results of a multiparametric study. Breast Cancer Res Treat 1995, 36:205–217